

# Generalized Rotational Moment Invariants For Robust Object Recognition

Vazeerudeen Abdul Hameed, and Siti Mariyam Shamsuddin

*Soft Computing Research Group*  
Faculty of Computing UniversitiTeknologi Malaysia, Skudai, Johor  
[vazeerudeen@yahoo.com](mailto:vazeerudeen@yahoo.com) & [mariyam@utm.my](mailto:mariyam@utm.my)

## Abstract

*High-order Hu moment invariant functions have always been required to solve a variety of problems. Up to this point, there was no generalized approach to extend the first six Hu moment invariants to higher orders. Therefore, this paper presents a generalized algorithm to determine rotationally invariant Hu moment invariants of any desired order, which are invariant to scaling, translation and rotation. Rotation has been stated to be a vital transformation that causes the non-linear transformation of an image, unlike scaling and translation, which are linear transformations of an image. Invariance to linear transforms can be achieved with the raw moments. However, non-linear transformations such as rotation require a unique combination of the raw moments to nullify the effects of the rotation transform. The algorithm proposed in this paper enables us to identify this specific combination of moments of specific order to achieve rotational invariance. The correctness of the proposed algorithm has been verified with appropriate proofs. The performance of a sample of new moment invariant functions generated from the proposed algorithm has been appraised specifically for rotational invariance with sample image data.*

**Keywords:***Invariant, Moment, Rotation, Scaling, Skew, Transform, Translation.*

## 1 Introduction

Images contain large amounts of information, and much of the information that is presented in today's world is in the form of images. The processing and understanding of an image consists of several stages that include image acquisition, image enhancement, image restoration, image representation, image compression and object recognition. Object recognition, the end goal of image understanding, is often achieved through a sequence of operations on the image

that range from low- to high-level image processing. The image processing operations group regions into objects and the image is described in terms of the object properties (location, shape, size) and the relations between the objects. Object recognition continues to pose a challenge to researchers, although several methods for object recognition have been proposed [1-4]. The difficulty of object recognition often stems from the method's inability to cope with variability due to lighting, scale, or rotation of the images.

The work presented here builds on work that focused on representing an image with moment invariant functions. In particular, it extends Hu moment invariants [5] to higher-order invariants to ensure invariance to image rotation. From this point on, the paper is organized as follows. Section 2 explains the origin and the formulation of Hu moments. The invariant nature of the formulations to the scaling, translation and rotation transforms is discussed. Section 3 reviews a large number of applications of the original Hu moment invariants (limited to third-order invariants) [5]. This order limitation is the motivation of the presented work. Section 4 proceeds to remove this limitation and extends Hu's original invariants to higher orders. Section 5 presents the actual algorithm for generating new moment invariant functions that are invariant to scaling, translation and rotation. Section 6 presents a sample of the new rotationally invariant moment invariant functions identified from the proposed algorithm in Section 5. Section 7 addresses the problem of polynomial dependency among the geometric moments and presents a solution to prevent it. Finally, Section 8 provides experimental results obtained from using the newly identified moment invariant functions in Section 6. The rotational invariance of these moment invariants is demonstrated and compared for different invariants.

## 2 History of invariants

Moment invariants have a long history that dates back to the theory of algebraic invariants studied by the German mathematician David Hilbert [6]. In an image, assume that  $f(x, y) \geq 0$  represents the image at the pixel  $(x, y)$ . The moment  $M_{pq}$  of order  $r$  of  $f(x, y)$  is defined as

$$M_{pq} = \iint P_{pq}(x, y) f(x, y) dx dy \quad (1)$$

where  $p \geq 0, q \geq 0$ , and  $P_{pq}$  is a polynomial basis function. The polynomial basis function could be an orthogonal function or a non-orthogonal function. Non-orthogonal moment functions are also called *geometric moment functions*, and a number of polynomial basis functions could be selected. The Hu moment invariants were generated with non-orthogonal polynomial basis functions as shown in equation (2). The raw moment functions were further normalized into central moments (3) that were invariant to translation.

### 3 Generalized Rotational Moment Invariants

$$m_{pq} = \iint_{x,y} x^p y^q f(x, y) dx dy \quad (2)$$

$$n_{pq} = \iint_{x,y} (x-x')^p (y-y')^q f(x, y) dx dy \quad (3)$$

Hu [5] defined seven moment invariants of second and third order, shown in equation (4).

$$\begin{aligned} I_1 &= n_{20} + n_{02} \\ I_2 &= (n_{20} - n_{02})^2 + (2n_{11})^2 \\ I_3 &= (n_{30} - 3n_{12})^2 + (3n_{21} - n_{03})^2 \\ I_4 &= (n_{30} + n_{12})^2 + (n_{21} + n_{03})^2 \\ I_5 &= (n_{30} - 3n_{12})(n_{30} + n_{12})[(n_{30} + n_{12})^2 - 3(n_{21} + n_{03})^2] \\ &\quad + (3n_{21} - n_{03})(n_{21} + n_{03})[3(n_{30} + n_{12})^2 - (n_{21} + n_{03})^2] \\ I_6 &= (n_{20} - n_{02})[(n_{30} + n_{12})^2 - (n_{21} + n_{03})^2] + 4n_{11}(n_{30} + n_{12})(n_{21} + n_{03}) \\ I_7 &= (3n_{21} - n_{03})(n_{30} + n_{12})[(n_{30} + n_{12})^2 - 3(n_{21} + n_{03})^2] \\ &\quad - (n_{30} - 3n_{12})(n_{21} + n_{03})[3(n_{30} + n_{12})^2 - (n_{21} + n_{03})^2] \end{aligned} \quad (4)$$

Each of the Hu moment invariants of the equations in equation (4) is invariant to rotation, scaling and translation. In addition,  $I_7$  is also invariant to skew. When represented in polar form, the geometric invariants, called *rotational moments*, ensure that an increase in the invariant order does not decrease the magnitude of the invariant. Boyce and Hossack [7] had derived rotational moments of arbitrary order that are shown to be invariant to rotation, scaling and intensity.

### 3 Work related to Hu's moment invariants

The robustness of the Hu moment invariant functions over the boundaries of images has been recently studied in [8], where it was shown that object recognition and discrimination could be achieved with better accuracy using Hu moments when they are applied over the boundary of a region in the image. The experiments shown in [8] involved identifying different shapes of keys that had minor differences in their shapes. An effective algorithm for the detection and description of image shape features based on  $I_7$  used in combination with a connected component analysis has been proposed in [9].

Hu moment invariants were used to reduce the translation, deflection and scale variations of welding images caused by welding deformations in [10]. All the seven moment invariants of the welding pool image were used to construct a similarity measure that was subsequently used to classify the images, achieving an

accuracy of 99%. An effective measure of shape circularity based on Hu moments is developed in [11], and all the seven Hu moment invariants were used in a biometric application for palm print identification in [12]. Hu moments were used in another biometric application, iris recognition [13], resulting in a False Acceptance Rate of 0.0% and a False Rejection Rate of 2.5%.

Hu moment invariants have also been used to determine defects in wood with 86% accuracy [14] and to process Synthetic Aperture Radar (SAR) images [15], where the existing seven Hu moment invariants in combination with the Support Vector Machine (SVM) over the SAR images achieved 96.18% accurate identification of target objects. Work performed on 3D shape retrieval, as reported in [16], also emphasizes the use of Hu moment invariants for the compact representation of multi-view descriptors. Texture analysis over a spermatozoa data set was performed by researchers in [17]. They found that the Hu moment invariants had poor performance as global descriptors. However there existed only seven Hu moment invariants for the researchers to use. This paper proposes a generalized algorithm to determine new Hu moment invariants which could be used in such research in future. Table 1 summarizes the applications of the Hu moments discussed above. Column 2 lists the drawbacks reported in these applications, while column 3 suggests the expected improvements afforded by the use of higher-order Hu invariants.

Table 1: Improvements in research that could be accomplished through the proposed work

Reference	Important drawbacks	Impact of proposed algorithm
HaiFeng Zhang et. al. [8]	Hu moments $I_1 - I_7$ were found to be computationally complex; therefore, only the boundary of shapes were evaluated. However, this approach reduces discrimination caused by loss of information.	The larger number of moment invariants identified by the proposed algorithm provides a choice that can reduce the number of invariants to be computed and thus reduce computational complexity.
Xiuxin Chen et. al. [9]	The authors were successful in discriminating the objects. However, the experimental results in this work have a large deviation in the measures for the first three Hu moment invariants of a given object.	Higher-order moment invariants as achieved in this paper could be used to minimize the impact of scaling and achieve a more accurate identification of objects.

## 5 Generalized Rotational Moment Invariants

<p>GaoFeiet. al. [10] Jin Soo NOH et. al. [12]</p>	<p>As found in many other works, all the seven Hu moment invariants have been used in the experiment. No selection of invariants has been made, resulting in a computational complexity that is large.</p>	<p>As more moment invariant functions become available, a careful choice from the infinitely large source could achieve better performance with less computation.</p>
<p>JovisaZunic et. al. [11] ReinhardKlette et. al. [18]</p>	<p>The shape circularity measure for real-time applications could not be effectively computed due to the discrete nature of images [11]. A descriptor based on the asymmetries in the distribution of roughness (ADR) as in [18] used only moment invariants of second order.</p>	<p>Higher-order moment invariants work better over circularly symmetric objects and in asymmetric scenarios. Hence, as new higher-order moment invariants are produced, the shape analysis as accomplished in this work could be significantly improved.</p>
<p>Hongbo Mu et. al. [14]</p>	<p>The authors have directly used the improved shape descriptors given in [19].</p>	<p>The work of [19] could be generalized over the new moment invariant functions identified by the proposed method to achieve a higher degree of accuracy with less computational complexity.</p>
<p>Oscar Garcia-Olalla et. al. [17]</p>	<p>Texture analysis was conducted with several descriptors which include Hu moment invariants. The invariants proved to be less accurate.</p>	<p>The accuracy of the representation heavily depends on the precision of the moments used. Therefore, the results can be further improved with the higher-order moment invariants proposed in this research.</p>
<p>Fu Yan et. al. [15]</p>	<p>More training for the SVM is required, as is apparent in the experiment. The seven Hu moments have all been computed instead of selecting the few necessary, increasing the</p>	<p>A careful selection of moment invariants could be made from the proposed algorithm that would reduce both the computational complexity and the training for the</p>

## 4 An analysis of the existing extensions to the Hu moment invariants

Work done in [20] explains that the Hu invariants were limited to third-order and that the Hu invariants  $I_2$  and  $I_3$  shown in equation (4) are dependent on the polynomial used in the integral. This dependency between the invariants reduces their contribution to pattern recognition. A missing invariant  $I_8$  of order three defined in equation (5) was also found [20]. However, as shown in [21], it is essential to find a method to generate Hu-like moment invariants of higher orders.

$$I_8 = n_{11}[(n_{30} + n_{12})^2 - (n_{03} + n_{21})^2] - (n_{20} - n_{02})(n_{30} - n_{12})(n_{03} - n_{21}) \quad (5)$$

The need for higher-order moments also follows from the rotational symmetry of the objects of interest. An object that is symmetric to rotation requires invariants involving higher-order moments to achieve clearly distinct invariant measures. The symmetry also causes moments of different orders to have identical values. Complex invariants constructed with higher-order moments up to order five were used to distinctly identify rotationally symmetric objects [20]. As stated in [20], we find that the lower-order complex moments are less sensitive to noise than the higher-order moments. Therefore, complex moment invariants were usually limited to lower-order moments. The number of folds of symmetry ( $N$ ) was used as an important factor in deciding the threshold. Although complex moments are sensitive to noise at higher orders, the geometric moments of higher orders are still capable of identifying objects with rotational symmetry. Moreover, there has been no specific limitation of the order of moments involved in the computation of invariants. However, it is difficult to know the exact highest order of the moment required for any object with rotational symmetry of order  $N$ . Authors in [20] had proposed a graph-based algorithm to determine skew moment invariant functions. However, this paper presents a generalized algorithm to determine higher-order rotational moment invariant functions.

The effect of the rotation and scaling of images on Hu moment invariants has been studied in [22]. The discrete nature of the image affects the invariance of the Hu moment invariants. A compromise between the spatial resolution of the image and computational speed can help achieve better invariance of the existing seven Hu moment invariants. The algorithm proposed in this paper expands the number of new moment invariants, thereby overcoming the impact of the rotation of discrete images. An integrated formulation of United Moment and Aspect Moment into Zernike Moment Invariant [23] accomplishes an intra-class and inter-class analysis of the character images. Issues with the use of geometric

## 7 Generalized Rotational Moment Invariants

scaling of Hu moments were reported, leading to a combination of the different moment formulations for the effective analysis of character images. Unlike geometric moment invariants such as Hu moments, we find a number of contributions towards the betterment of orthogonal moment invariants such as Zernike moments [24-25]. Thus, based on the above observations, it can be observed that the Hu moment invariants often had to be combined with other formulations to improve their performance. This is mainly due to the lack of higher-order Hu moment invariant functions. The generalized algorithm presented in this paper will resolve this problem to determine higher-order, rotational Hu-like moment invariant functions.

## 5 An algorithm to determine rotational Hu moment invariants of higher order

The algorithm to obtain higher-order Hu moment invariants proposed in this paper consists of the following:

Input: order of the moment invariant  $p + q$  ; degree of the invariant function  $r$

Output: moment invariant of order  $p + q$

Step 1: Generate all possible product combinations of raw moments  $m_{p_1q_1}, m_{p_2q_2}, \dots, m_{p_rq_r}$  such that both  $p_1 + p_2 + \dots + p_r$  and  $q_1 + q_2 + \dots + q_r$  are always even.

Step 2: Create the sum-of-products expression

$$I = k_1 m_{1p_1q_1} m_{1p_2q_2} \dots m_{1p_rq_r} \\ + k_2 m_{2p_1q_1} m_{2p_2q_2} \dots m_{2p_rq_r} + \dots \\ + k_n m_{np_1q_1} m_{np_2q_2} \dots m_{np_rq_r}$$

Step 3: Identify the values of the constants  $k_1, k_2, \dots, k_n$  such that the function  $I$  is invariant to the transformation  $u = x \cos \theta - y \sin \theta$  and  $v = x \sin \theta + y \cos \theta$  for an image function  $f(x, y)$  with a single co-ordinate.

The rationale behind the definition of the steps in the above algorithm can be understood from the following proofs.

**Pythagorean Identity:**  $\sin^2 \theta + \cos^2 \theta = 1$

Image rotation involves pixel relocation as a function of Sine and Cosine. The above Pythagorean identity has been used to enable the moment invariant function to be invariant to rotation. In Step 1 of the algorithm above, the moment products

are chosen such that  $\sum_{i=1}^r p_i$  and  $\sum_{i=1}^r q_i$  are even. This enables the exponents of the Sine and Cosine functions in the moments  $m_{pq}$  to always be a multiple of two, so the Pythagorean identity can be satisfied and the impact of rotation can be removed.

**Lemma:** *If a moment invariant function is invariant to rotation of an image function  $f(x,y)$  at a single co-ordinate, then it is also invariant for an image function  $f'(x,y)$  at many co-ordinates.*

**PROOF:** Upon rotation by an angle  $\theta$ , the pixel  $(x, y)$  of an image is in the position  $(u, v)$  determined by

$$\begin{aligned} u &= x \cos \theta - y \sin \theta \\ v &= x \sin \theta + y \cos \theta \end{aligned} \quad (6)$$

Rotation is very different from other image transformations. For example, scaling or translation causes all the pixels to change their location by a linear constant, whereas rotation causes pixels that are farther from the center of the rotation to move exponentially larger distances than those that are nearer to the center. Thus, when the image is rotated by angle  $\theta$  with respect to the origin  $(0,0)$ , the moment  $m_{pq}$  of equation (2) becomes

$$m_{pq} = \iint x^p y^q f((x \cos \theta - y \sin \theta), (x \sin \theta + y \cos \theta)) dx dy \quad (7)$$

That is, it transforms  $f(x, y)$  into  $f(x \cos \theta - y \sin \theta, x \sin \theta + y \cos \theta)$ .

However, the effect of rotation can be viewed in a different perspective by leaving the image in its original position and allow the axes to rotate in the opposite direction, causing the same impact on the pixels of the image. Figure 1 illustrates this process: Figure 1(a) shows two pixels at locations  $(0,0)$  and  $(3,3)$ , respectively. Upon a counter-clockwise rotation with  $(0,0)$  as the center and  $\theta = 60^\circ$ , these pixels are relocated to  $(0,0)$  and  $(-1,4)$  as shown in Figure 1(b). Rotating the axes clock-wise by  $\theta = 60^\circ$  leaves the two pixels in their original relative positions, as shown in Figure 1(c) and Figure 1(d).

Thus, the rotation transform can be applied on the co-ordinates instead of the pixel values.

Hence Eq. (7) can be rewritten as

$$m_{pq} = \iint (x \cos \theta - y \sin \theta)^p (x \sin \theta + y \cos \theta)^q f(x, y) dx dy \quad (8)$$

where the moment function is now a function of variables

9 Generalized Rotational Moment Invariants

$x, y$  and  $\theta$ . Using

$$\begin{aligned} u &= x \cos \theta - y \sin \theta \\ v &= x \sin \theta + y \cos \theta \end{aligned} \tag{9}$$

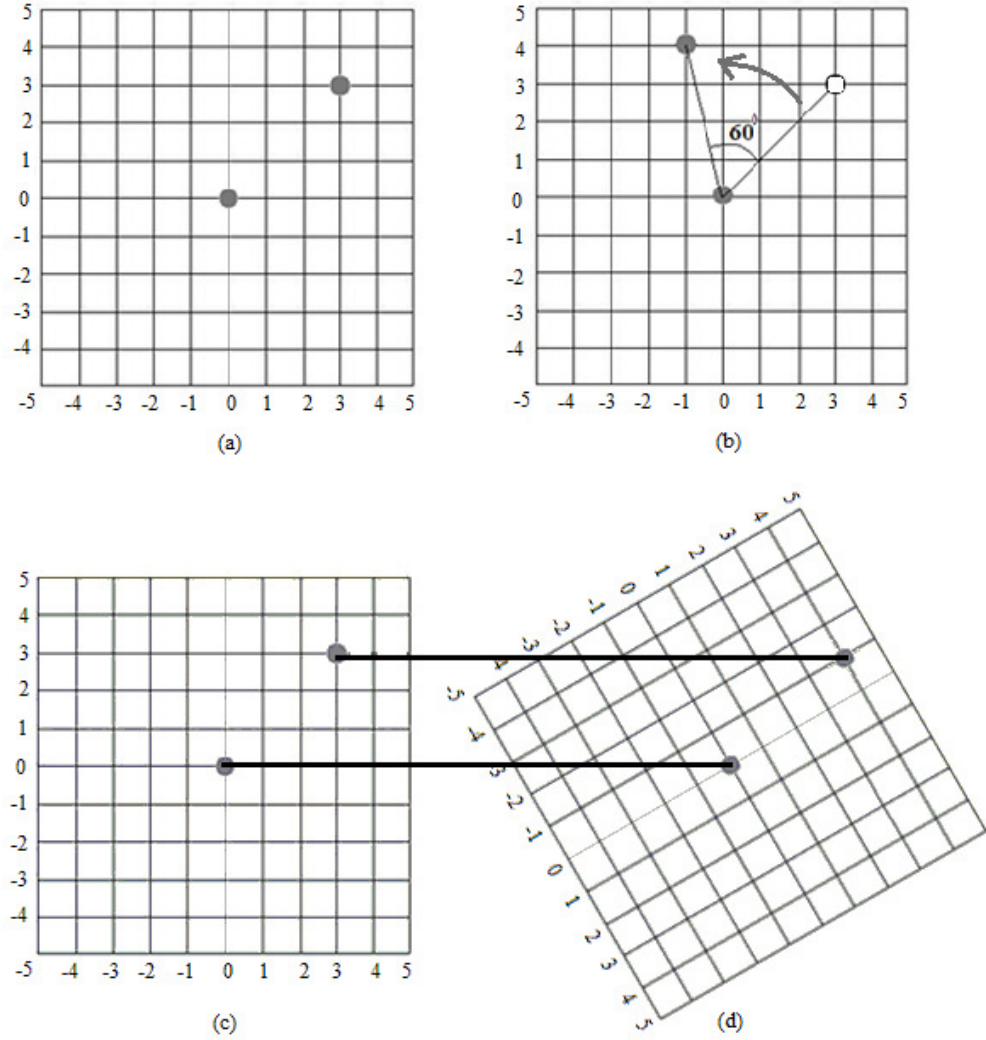


Fig. 1. Impact of rotation transform over the pixels in an image. (a) Original location of two points on an image. (b) Rotation of the image about the centre. (c) Original location of two points on an image as in Fig. 1(a). (d) Rotation of the frame to achieve the effect of rotation in Fig. 1(b)

Eq. (8) becomes,

$$m_{pq} = \iint u^p v^q f(x, y) dx dy \tag{10}$$

which, upon a change of variables according to Eq. (9), whose Jacobian is

$$J(x, y) = \begin{vmatrix} \frac{\partial u}{\partial x} & \frac{\partial u}{\partial y} \\ \frac{\partial v}{\partial x} & \frac{\partial v}{\partial y} \end{vmatrix} = 1 \quad (11)$$

becomes

$$m_{pq} = \iint u^p v^q f(x, y) dudv. \quad (12)$$

For a two-dimensional function image  $f(x, y)$ , the absolute value of the Jacobian measures the amount of stretching or deformation undergone by the image due to the transformation. Therefore, according to Eq. (11) above, rotation is a transformation that does not cause loss or damage to the image data. Moreover, because  $J(x, y) \neq 0$ , it follows that the rotation transform is invertible.

As shown in Eq. (12), the integral function is not affected by the change of variables induced by rotation. Therefore, every individual pixel is independently affected by rotation uniformly. Hence, if a moment invariant function is invariant to the rotation of an image function  $f(x, y)$  at a single coordinate, then it is also invariant to the rotation of an image  $f(x, y)$  composed of several pixels. Hence, it is proved.

This lemma is used in Steps 2 and 3 of the algorithm. In Step 2 of the algorithm, a sum-of-products expression is formed to enable the moments to nullify the presence of the Sine and Cosine functions introduced due to rotation. However, in this step, each moment product  $m_{np1q1} m_{np2q2} \dots m_{nprqr}$  is associated with a constant  $k_n$ . The invariant function I in Step 2 must now be solved to determine the values of  $k_1, k_2 \dots k_n$ . The lemma proves that it is enough to solve the function I for an image  $f(x, y)$  at a single co-ordinate subject to rotation by an angle  $\theta$ . The advantage of this approach is that, because we consider an image  $f(x, y)$  at a single pixel, the integration function in Eq. (1) disappears and the function I in the algorithm becomes a polynomial to be solved.

The following example verifies the use of the algorithm to determine an existing Hu moment invariant as follows.

Input: Order  $(p + q) = 2$ , Degree=1

Step 1:  $m_{20}, m_{11}, m_{02}$

Step 2:  $I = k_1 m_{20} + k_2 m_{11} + k_3 m_{02}$

Step 3: Applying the rotation transform over the moments for I we have,

## 11 Generalized Rotational Moment Invariants

$$I = k_1 \sum_x \sum_y (x \cos \theta - y \sin \theta)^2 f(x, y) +$$

$$k_2 \sum_x \sum_y (x \cos \theta - y \sin \theta)(x \sin \theta + y \cos \theta) f(x, y)$$

$$k_3 \sum_x \sum_y (x \sin \theta + y \cos \theta)^2 f(x, y)$$

For  $k_1 = 1, k_2 = 0, k_3 = 1$  we have

$$I = \sum_x \sum_y (x^2 + y^2) f(x, y).$$

Hence

$$I = m_{20} + m_{02}.$$

The raw moments  $m_{20}, m_{02}$  can be replaced by central moments  $n_{20}, n_{02}$ . Hence, we have

$$I = n_{20} + n_{02} \quad (13)$$

We can similarly derive the remaining Hu moment invariants.

## 6 New Moment Invariant Functions

In this section, we derive a sample of three new rotation invariants as an extension to the existing Hu moment invariant functions. The new invariants were identified in accordance with the algorithm proposed in this paper.

Let  $n_{pq}^r = \left[ \sum_x \sum_y x^p y^q f(x, y) \right]^r$  be the central moment function of order

$(p + q)$  and degree  $r$ . Then, for a given order  $(p + q)$  and order  $r$ , the following are the sample moment invariant functions.

**Sample Invariant  $I_a$**

Input: Order  $(p + q) = 2$ , Degree  $(r) = 2$

Step 1:  $m_{20}m_{20}, m_{20}m_{02}, m_{11}m_{11}, m_{02}m_{02}$

Step 2:  $I_a = k_1 m_{20}m_{20} + k_2 m_{20}m_{02} + k_3 m_{11}m_{11} + k_4 m_{02}m_{02}$

Step 3: Applying the rotation transform over the moments for  $I_a$ , we have

$$\begin{aligned}
 I_a = & k_1 \left[ \sum_x \sum_y (x \cos \theta - y \sin \theta)^2 f(x, y) \right]^2 + \\
 & k_2 \left[ \sum_x \sum_y (x \cos \theta - y \sin \theta)^2 f(x, y) \right] \left[ \sum_x \sum_y (x \sin \theta + y \cos \theta)^2 f(x, y) \right] + \\
 & k_3 \left[ \sum_x \sum_y (x \cos \theta - y \sin \theta)(x \sin \theta + y \cos \theta) f(x, y) \right]^2 + \\
 & k_4 \left[ \sum_x \sum_y (x \sin \theta + y \cos \theta)^2 f(x, y) \right]^2
 \end{aligned}$$

For  $k_1 = 1, k_2 = 0, k_3 = 2, k_4 = 1$  we have

$$I_a = \sum_x \sum_y (x^2 + y^2)^2 (f(x, y))^2$$

Hence,

$$I_a = m_{20}m_{20} + 2m_{11}m_{11} + m_{02}m_{02}$$

Step 4: Replacing the raw moments  $m_{20}, m_{11}, m_{02}$  with central moments  $n_{20}, n_{11}, n_{02}$ , we have

$$I_a = n_{20}^2 + 2n_{11}^2 + n_{02}^2 \quad (14)$$

**Sample Invariant  $I_b$**

Input: Order  $(p + q) = 3$ , Degree  $(r) = 2$

Step 1:  $m_{30}m_{30}, m_{30}m_{12}, m_{03}m_{21}, m_{03}m_{03}$

Step 2:  $I_b = k_1 m_{30}m_{30} + k_2 m_{03}m_{03} + k_3 m_{30}m_{12} + k_4 m_{03}m_{21}$

Step 3: Applying the rotation transform over the moments for  $I_b$ , we have

### 13 Generalized Rotational Moment Invariants

$$\begin{aligned}
 I_b = & k_1 \left[ \sum_x \sum_y (x \cos \theta - y \sin \theta)^3 f(x, y) \right]^2 + k_2 \left[ \sum_x \sum_y (x \sin \theta + y \cos \theta)^3 f(x, y) \right]^2 \\
 & k_3 \left[ \sum_x \sum_y (x \cos \theta - y \sin \theta)^3 f(x, y) \right] \\
 & \left[ \sum_x \sum_y (x \cos \theta - y \sin \theta)(x \sin \theta + y \cos \theta)^2 f(x, y) \right] + \\
 & k_4 \left[ \sum_x \sum_y (x \sin \theta + y \cos \theta)^3 f(x, y) \right] \\
 & \left[ \sum_x \sum_y (x \cos \theta - y \sin \theta)^2 (x \sin \theta + y \cos \theta) f(x, y) \right]
 \end{aligned}$$

For  $k_1 = 1, k_2 = 1, k_3 = 3, k_4 = 3$  we have

$$I_b = \sum_x \sum_y (x^2 + y^2)^3 (f(x, y))^2$$

Hence

$$I_b = m_{30}^2 + 3m_{30}m_{12} + 3m_{03}m_{21} + m_{03}^2$$

Step 4: Replacing the raw moments  $m_{30}, m_{12}, m_{21}, m_{03}$  with central moments  $n_{30}, n_{12}, n_{21}, n_{03}$ , we have

$$I_b = n_{30}^2 + 3n_{30}n_{12} + 3n_{03}n_{21} + n_{03}^2 \quad (15)$$

**Sample Invariant  $I_c$**

Input: Order  $(p + q) = 4$ , Degree  $(r) = 1$

Step 1:  $m_{40}, m_{22}, m_{04}$

Step 2:  $I_c = k_1 m_{40} + k_2 m_{22} + k_3 m_{04}$

Step 3: Applying the rotation transform over the moments for  $I_c$ , we have

$$\begin{aligned}
 I_c = & k_1 \left[ \sum_x \sum_y (x \cos \theta - y \sin \theta)^4 f(x, y) \right] + \\
 & k_2 \left[ \sum_x \sum_y (x \cos \theta - y \sin \theta)^2 (x \sin \theta + y \cos \theta)^2 f(x, y) \right] + \\
 & k_3 \left[ \sum_x \sum_y (x \sin \theta + y \cos \theta)^4 f(x, y) \right]
 \end{aligned}$$

For  $k_1 = 1, k_2 = 2, k_3 = 1$  we have

$$I_b = \sum_x \sum_y (x^2 + y^2)^2 f(x, y)$$

Hence

$$I_c = m_{40} + 2m_{22} + m_{04}$$

Step 4: Replacing the raw moments  $m_{40}, m_{22}, m_{04}$  with central moments  $n_{40}, n_{22}, n_{04}$ , we have

$$I_c = n_{40} + 2n_{22} + n_{04} \quad (16)$$

### Sample Invariant $I_d$

In accordance with the algorithm proposed in the paper and the steps shown for the generation of moment invariants  $I_a, I_b, I_c$ , the following invariant  $I_d$  was also generated. The steps for the generation of this invariant has been eliminated as they are similar to the steps used to generate  $I_a, I_b, I_c$ . This invariant  $I_d$  is of Order  $(p+q) = 4, 2$  and Degree  $(r) = 2$ .

$$I_d = n_{22}(n_{60}^2 + n_{06}^2) / 7 + n_{51}^2(n_{20} + 3n_{02}) + n_{15}^2(n_{02} + 3n_{20}) + 5n_{42}^2 n_{02} \quad (17)$$

## 7 Selection of Moment Invariant Functions

A common drawback of the geometric moment invariant functions is that there is no generalized invariant function identification method that has been addressed in this research. However, geometric moment invariants in general suffer from dependency between the functions. This problem also occurs in our proposed algorithm, such that we might generate moment invariant functions that are dependent upon the polynomials used in the integral. The following example explains such a dependency.

Consider the Hu moment invariants  $I_1, I_2$  from Eq. 4 and the proposed invariant  $I_c$  from Eq. 16. We find polynomial dependency between them, as follows.

$$I_1 = n_{20} + n_{02}$$

$$I_2 = (n_{20} - n_{02})^2 + 4n_{11}^2$$

$$I_c = n_{20}^2 + n_{02}^2 + 2n_{20}n_{02}$$

$$I_c = \frac{I_1^2 + I_2}{2}$$

The independence of the moment invariant functions is a necessary criterion to ensure that we do not measure the same invariant functions, which would contribute no additional information. Apart from the brute-force technique, no

## 15 Generalized Rotational Moment Invariants

technique exists to identifying polynomial dependencies between groups of functions. A polynomial dependency between moment invariant functions is said to exist when an invariant can be determined from one or more of the other invariant functions. Although we may not be able to determine the existence of a polynomial dependency, we could determine a group of moment invariant functions that would be selectively formed to avoid the dependency.

One important characteristic of moment functions can be used to prevent moment invariant functions that may suffer from polynomial dependencies. For any two moment functions  $n_{pq}$  and  $n_{rs}$ , we find that  $n_{pq} \neq n_{rs}$  for  $p \neq r$  and/ or  $q \neq s$ . This can be proven using the Johann Faulhaber's formula in Eq. (18), as follows.

$$\sum_{x=1}^n x^p = 1^p + 2^p + 3^p + \dots + n^p = \frac{1}{p+1} \sum_{i=0}^n (-1)^i \binom{p+1}{i} C_i B_i n^{p+1-i} \quad (18)$$

Consider any two moment functions  $n_{pq}$  and  $n_{ps}$ . For an image  $f$  with centroid (0,0) and all pixels of constant amplitude  $\rho$ , the moments would be evaluated as in Eq. (19). From the equations, we observe that the moments  $n_{pq} \neq n_{ps}$  for  $q \neq s$ . This is a simple proof that lets us understand that  $n_{pq} \neq n_{rs}$  for  $p \neq r$  and/ or  $q \neq s$ .

$$\begin{aligned} n_{pq} &= \sum_{x=1}^n x^p \rho \sum_{y=1}^m (y)^q = \sum_{x=1}^n x^p \frac{\rho}{q+1} \sum_{i=0}^m (-1)^i \binom{q+1}{i} C_i B_i m^{q+1-i} \\ n_{ps} &= \sum_{x=1}^n x^p \rho \sum_{y=1}^m (y)^s = \sum_{x=1}^n x^p \frac{\rho}{s+1} \sum_{i=0}^m (-1)^i \binom{s+1}{i} C_i B_i m^{s+1-i} \end{aligned} \quad (19)$$

Consider the invariants  $I_1$  from Eq. 4 and the proposed invariants  $I_a$  from Eq. 14 and  $I_c$  from Eq. 16 which are all rotationally invariant.

$$\begin{aligned} I_1 &= n_{20} + n_{02} \\ I_c &= n_{20}^2 + n_{02}^2 + 2n_{20}n_{02} \\ I_c &= I_1^2 \\ I_a &= n_{20}^2 + n_{02}^2 + 2n_{11}^2 \end{aligned}$$

$I_a$  is another invariant similar to  $I_c$  in structure, but  $I_a$  is independent of  $I_1$ . This is feasible because the invariants are not formed from the exact same moment functions. One important characteristic of this solution to eliminating polynomial dependency is that we will obtain false negatives that could eliminate certain independent invariants. The three sample invariants  $I_a$ ,  $I_b$ ,  $I_c$  and  $I_d$  proposed in this paper are clearly independent of each other. Similarly a set of seven new fully independent rotational moment invariants have been presented in Appendix A.

these invariants were generated from the algorithm proposed in Section 6 of this paper.

## 8 Experimental Analysis

The invariants identified in Section 6 of this paper were tested for two different scenarios, as follows. Firstly, the invariants were tested over circularly symmetric geometric shapes, and the performance of the invariants was appraised. Secondly, the proposed invariants were used to perform object matching in the real world. The two cases of the experiments are as follows.

### Case 1: An analysis on polygon images

This experiment was designed to experimentally understand the rotationally invariant nature of the identified invariants and to determine the discriminatory ability of the identified invariants. To accomplish these objectives, we used monochrome bitmap images of polygons. Such polygon images are said to contain very little information because the only feature that differentiates the polygons is the number of sides.

The polygons chosen for the experiment were a triangle (P3), square (P4), pentagon (P5), hexagon (P6), heptagon (P7), octagon (P8), nonagon (P9) and circle (Pc), as shown in Figure 2. These polygons had an approximate radius of 60 pixels. Each of the shapes was rotated at twelve different angles of 0, 30, 45, 60, 90, 120, 150, 180, 200, 270, 300 and 330 degrees, and the moment invariant  $I_a$  as derived in Section 6 above was evaluated. The measures are presented in Table 2. The table presents the percentage standard deviation in the measure of the invariant for every shape rotated at the twelve different angles. The percentage standard deviation is less than 1% in all the shapes, which gives experimental proof of the invariance of  $I_a$  to rotation. Hence, our first objective as proposed above could be verified.

Further, an ANOVA test was performed between every two consecutive shapes. This is necessary because every consecutive shape, such as triangle and square or square and pentagon, differs from the previous shape by an increase of one side, which is a minimal difference in feature that causes the shapes to look different. The ANOVA test results are presented in Table 3. For every pair of shapes in Table 3, we find that the SS (Sum of Squares) Variation within the group (WG) is always less than that between the groups (BG). The same characteristic is reflected in the MS (Mean Square) Variation measures. The test statistic (F) has been found to be larger than the critical value (F-Crit) for all pairs of shapes, as observed in the table. This is a very important measure that explains us that the  $I_a$



Table 3: ANOVA test of  $I_a$  measure for every pair of adjacent polygons

<i>Polygon Pair</i>	<i>Source of Variation</i>	<i>SS</i>	<i>df</i>	<i>MS</i>	<i>F</i>	<i>Probability</i>	<i>F crit</i>
P3-P4	BG	1.75E+28	1	1.75E+28	132554.2	4.42E-43	4.3
	WG	2.9E+24	22	1.32E+23			
	Total	1.75E+28	23				
P4-P5	BG	8.05E+27	1	8.05E+27	43562.98	9.12E-38	4.3
	WG	4.07E+24	22	1.85E+23			
	Total	8.06E+27	23				
P5-P6	BG	6.29E+27	1	6.29E+27	1055.935	4.35E-20	4.3
	WG	1.31E+26	22	5.96E+24			
	Total	6.42E+27	23				
P6-P7	BG	3.39E+27	1	3.39E+27	553.1598	4.39E-17	4.3
	WG	1.35E+26	22	6.13E+24			
	Total	3.53E+27	23				
P7-P8	BG	2.22E+27	1	2.22E+27	2278.748	1.03E-23	4.3
	WG	2.14E+25	22	9.73E+23			
	Total	2.24E+27	23				
P8-P9	BG	3.09E+26	1	3.09E+26	336.3224	8.09E-15	4.3
	WG	2.02E+25	22	9.2E+23			
	Total	3.3E+26	23				
P9-Pc	BG	9.01E+27	1	9.01E+27	15648.62	7.03E-33	4.3
	WG	1.27E+25	22	5.76E+23			
	Total	9.03E+27	23				

### Case 2: An Analysis on alphabet blocks

This experiment was designed to experimentally understand the performance of the invariants identified in this paper for real-world scenarios. In this experiment, we created a sample database of 15 alphabet blocks. A sample alphabet block “B” is shown in Figure 3. The alphabets were chosen such that there was little difference in their features. For example the alphabets “M” and “W” are approximately the same character that has been flipped vertically. Similarly, the alphabets “O” and “Q” have only a small feature to differentiate them. The 15 alphabet images were pre-processed in MATLAB to refine them by eliminating random noise that occurred during the acquisition. The invariants  $I_b$  and  $I_c$  were measured for these character blocks and stored in the database.

## 19 Generalized Rotational Moment Invariants

Pictures of randomly scabbled alphabet blocks as shown in Figure 4 were captured to subject them to alphabet recognition using the database of 15 alphabets that we had created. Image pre-processing was also applied on these scabble images to eliminate noise. The alphabet recognition was performed over the boundaries to achieve invariance to color and illumination. Therefore, we used Canny's edge detector to determine the boundaries of the alphabets. Figure 5 shows the edge-detected version of Figure 4. An advantage of the Canny's edge detector was that the boundaries that were found were connected the most frequently, as shown in Figure 5. This helped us to further perform region-growing image segmentation to segment the alphabets from the scabble. The segmented alphabets were subjected to the measure of invariants  $I_b$  and  $I_c$ .

Five different trials of the experiment in which the scabble was changed randomly were conducted. The obtained values of  $I_b$  and  $I_c$  over the five trials were plotted as shown in Figure 6. As evident in the graph, there was a sufficient degree of clustering in the measures over the five trials. There was no error in classification except for those that had close boundaries in the moment measures. As shown in Figure 6, there was difficulty in classifying the letters B and Z due to their moment measures having close boundaries. There was deviation in the measures of other alphabets, as observed in Q, W, M and others. However, such clusters were significantly separated from each other and were therefore easily recognized.



Fig. 3. Sample alphabet recorded in the database



Fig. 4. Sample arrangement of alphabets used in the experiment



Fig. 5. Processed and edge detected form of Fig. 4

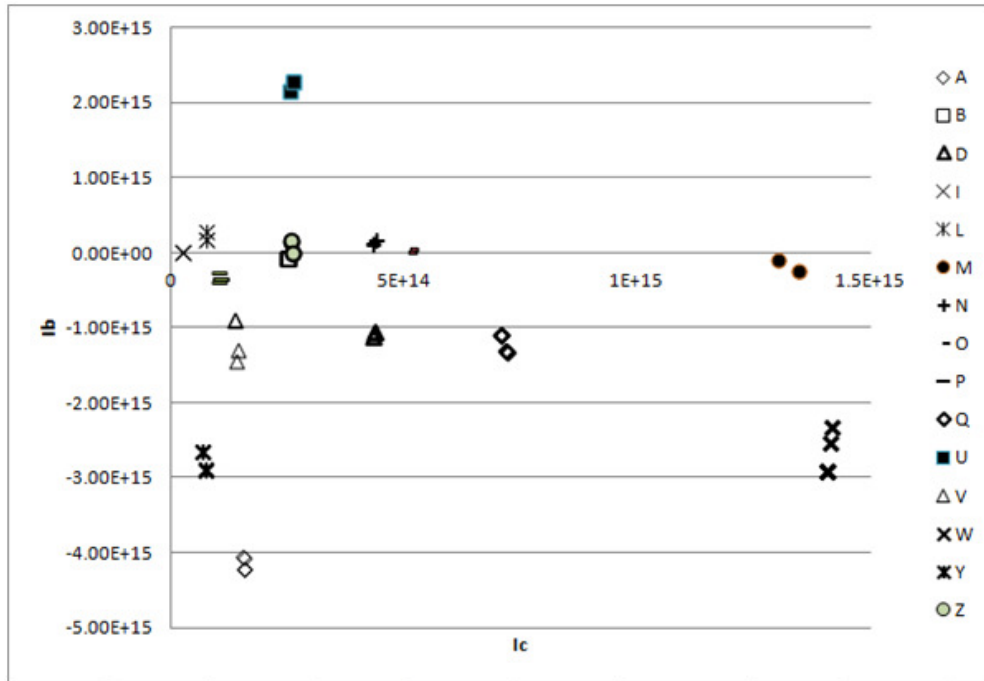


Fig. 6. Plot of the measure of invariants  $I_b$  and  $I_c$  for alphabet scrabbles in five different trials.

The experiments in Case 1 and Case 2 prove that the proposed invariants  $I_a$ ,  $I_b$  and  $I_c$  that were identified according to the algorithm proposed in Section 5 are invariant to rotation. The practical applicability of such invariants is apparent from the experiment in Case 2. However, we also find some discrepancy in the values of the moment invariants. This discrepancy shall be attributed to the discrete nature and the resolution of the images. Zhihu Huang and Jinsong Leng [22] presented a study on the effect of the rotation and scaling of images on Hu moment invariants. They concluded that rotation could cause discrepancies in the values of the Hu moment invariants. However, we observe that the discrepancy in the values is still minor and does not affect object recognition.

## 9 Conclusion

In this study, we have provided a generalized algorithm to extend the Hu moment invariant functions to any desired order and degree. As explained in this paper, there had been no specific algorithm to generalize the development of Hu moment invariants, unlike other orthogonal moment invariants [24-25]. Hence, our work has addressed this problem. This work has thus contributed to expanding the choice of Hu moment invariant functions and provided researchers with a

## 21 Generalized Rotational Moment Invariants

customized choice of moment invariants that could be suitable to solve a specific problem. The recognition and clear discrimination of circularly symmetric objects has been a challenge that was accomplished with suitable experiments in Section 8. The problem of the reduced ability of moment invariants was resolved in Section 7, providing a solution for researchers to choose independent moment invariant functions. The increased number of moment invariant functions of higher orders proposed in this paper could be used to achieve more accurate results for such problems. The correctness of the proposed algorithm was verified with mathematical proofs. A sample of the invariants generated from the proposed algorithm was also verified with sample images in two different experimental scenarios.

### Acknowledgments

The authors would like to thank the Universiti Teknologi Malaysia (UTM) for their support in Research and Development and the *Soft Computing Research Group* (SCRG) for the inspiration in making this study a success. This work is supported by The Ministry of Higher Education (MOHE) under the Long Term Research Grant Scheme (LRGS/TD/2011/UTM/ICT/03- 4L805).

### References

- [1] Rafael C Gonzalez, Richard E Woods. "Digital Image Processing", Prentice Hall; 3 edition, ISBN-10: 013168728X, 2007
- [2] K Mikolajczyk, C Schmid. A Performance Evaluation of Local Descriptors. *Pattern Analysis and Machine Intelligence*, IEEE Transactions on, **27**, 1615 – 1630 (2005)
- [3] J M Morel, G Yu. ASIFT: A New Framework for Fully Affine Invariant Image Comparison. *SIAM Journal on Imaging Sciences*, **2**, 438-469 (2009).
- [4] Wong Yee Leng & Siti Mariyam Shamsuddin. Writer Identification for Chinese Handwriting. *International Journal of Advances in Soft Computing and Its Applications*, **2**(2): 1-32 (2010).
- [5] M K Hu. Visual pattern recognition by moment invariants. *IRE Transactions on Information Theory*, **IT-8**, 179-187 (1962).

- [6] D Hilbert. Theory of Algebraic Invariants. Cambridge, U.K.: Cambridge Univ. Press, 1993.
- [7] J F Boyce and W J Hossack. Moment invariants for pattern recognition. Pattern Recognition Letters, **1**, 451-456, (1983).
- [8] H F Zhang, X Zhang. Shape recognition using a moment algorithm. Multimedia Technology (ICMT), International Conference on, 3226-3229 (2011).
- [9] Xiuxin Chen, ShiangWei, Suxia Xing, KebinJia. An effective image shape feature detection and description method. Mechatronic Science, Electric Engineering and Computer (MEC), International Conference on, 1957 – 1960 (2011).
- [10] Gao Fei, Wang Kehong. The research of classification method of arc welding pool image based on invariant moments. Power Engineering and Automation Conference (PEAM), IEEE, **3**, 73 - 76 (2011).
- [11] Jovisa, Kaoru Hirota, Paul L Rosin. A Hu moment invariant as a shape circularity measure. Pattern Recognition, **43**, 47-57 (2010).
- [12] Jin Soo NOH, Kang Hyeon RHEE. Palmprint Identification Algorithm using Hu Invariant Moments and Otsu Binarization. Proceedings of the Fourth Annual ACIS International Conference on Computer and Information Science (ICIS'05), 94-99 (2005)
- [13] S V Sheela, P A Vijaya. Non-linear Classification for Iris patterns. in Proceedings of the Multimedia Computing and Systems (ICMCS), International Conference Ouarzazate, Morocco, 1-5 (2011)
- [14] Hongbo Mu and Dawei Qi. Pattern Recognition of Wood Defects Types Based on Hu Invariant Moments. Image and Signal Processing, CISP'09 2nd International Congress, Tianjin, 1-5 (2009).
- [15] Fu Yan, Wang Mei, Zhang Chunqin. SAR Image Target Recognition Based on Hu Invariant Moments and SVM. in Proceedings of Fifth International Conference on Information Assurance and Security, IEEE Trans, 585-588 (2009).

## 23 Generalized Rotational Moment Invariants

- [16] Petros Daras, Apostolos Axenopoulos. A 3D Shape Retrieval Framework Supporting Multimodal Queries. *International Journal of Computer Vision*, **89**, 229-247 (2010).
- [17] Oscar García-Olalla, Enrique Alegre, Laura Fernández-Robles, María Teresa García-Ordás and Diego García-Ordás. Adaptive local binary pattern with oriented standard deviation (ALBPS) for texture classification. *EURASIP Journal on Image and Video Processing*, **31** (2013)
- [18] Reinhard Klette, Jovisa Zunic. ADR shape descriptor – Distance between shape centroids versus shape. *Computer Vision and Image Understanding*, **116**, 690-697 (2012)
- [19] Chaur-Chin Chen. Improved moment invariants for shape discrimination. *Pattern Recognition*, **26**, 683-686 (1993)
- [20] T Suk, J Flusser, Affine moment invariants generated by graph method. *Pattern Recognition*, **44**, 2047 – 2056 (2011)
- [21] S M Shamsuddin, M N Sulaiman, M Darus. Invarianceness of Higher Order Centralised Scaled-invariants Undergo Basic Transformations. *International Journal of Computer Mathematics*, **79**, 39-48 (2002).
- [22] Zhihu Huang and Jinsong Leng. Analysis of Hu's Moment Invariants on Image Scaling and Rotation. in *Proceedings of the Computer Engineering and Technology, 2nd International Conference Chengdu*, V7-476 - V7-480 (2010).
- [23] Norsharina Abu Bakar, Siti Mariyam Shamsuddin, and Aida Ali. An Integrated Formulation of Zernike Representation in Character Images. *IEA/AIE 2010, Part III, LNAI 6098*, 359–368 (2010)
- [24] Chandan Singh, EktaWalia, Rahul Upneja. Accurate calculation of Zernike moments. *Information Sciences*, **233**, 255-275 (2013)
- [25] Khalid M. Hosny. A systematic method for efficient computation of full and subsets Zernike moments. *Information Sciences*, **180**, 2299-2313 (2010)